LAWRENCE
LIVERMORE
NATIONAL
LABORATORY

LLNL-JRNL-412589

Time-Dependent Measure of a Nano-Scale Force-Pulse Driven by the Axonemal Dynein Motors in Individual Live Sperm Cells

M. J. Allen, R. E. Rudd, M. W. McElfresh, R. Balhorn

April 28, 2009

Nanomedicine

Disclaimer

Time-Dependent Measure of a Nano-Scale Force-Pulse Driven by the Axonemal Dynein Motors in Individual Live Sperm Cells

Short title: Direct measure of flagellar propulsion

Michael J. Allen, Ph.D.*[1], Robert E. Rudd, Ph.D.[†], Mike W. M[c]Elfresh, Ph.D.[‡] and Rod Balhorn, Ph.D. [§]

*Biometrology, 851 West Midway Avenue, Alameda California 94501

[†]Condensed Matter and Materials Division, [§]Biosciences and Biotechnology Division, Lawrence Livermore National Laboratory, Livermore California 94551

[‡]Department of Physics, University of California, Davis California 95616

Keywords: cantilever, flagellum, motility, sensor, propulsion

[1]Corresponding Author (Current Address):

Michael J. Allen, Ph.D.

Center for Nanomedicine

5841 S. Maryland Ave., MC-6080, Room W-221 (Attn: Charisse Hopkins)

The University of Chicago, Chicago IL 60637

Phone: 773-702-8838 Fax: 773-702-4941

Email: allen1@uchicago.edu

Sources of Support:

This work was performed through support from Biometrology to M.J.A.; and to R.E.R., M.W.M. and R.B. from the US Dept. of Energy by the Lawrence Livermore National Laboratory under Contract No. DE-AC52-07NA27344.

Word and character counts:

118 characters and spaces in title, 38 characters and spaces in short title, 166 words in abstract, total words in manuscript (incl. acknowledgements, references and figure legends): 4194

Abstract

Nano-scale mechanical forces generated by motor proteins are crucial to normal cellular and organismal functioning. The ability to measure and exploit such forces would be important to developing motile biomimetic nanodevices powered by biological motors for Nanomedicine. Axonemal dynein motors positioned inside the sperm flagellum drive microtubule sliding giving rise to rhythmic beating of the flagellum. This force-generating action makes it possible for the sperm cell to move through viscous media. Here we report new nano-scale information on how the propulsive force is generated by the sperm flagellum and how this force varies over time. Single cell recordings reveal discrete ~50 ms pulses oscillating with amplitude 9.8 +/- 2.6 nN independent of pulse frequency (3.5-19.5 Hz). The average work carried out by each cell is 4.6×10^{-16} J per pulse, equivalent to the hydrolysis of ~5,500 ATP molecules. The mechanochemical coupling at each active dynein head is ~2.2 pN/ATP, and ~3.9 pN per dynein arm, in agreement with previously published values obtained using different methods.

Background

During flagellar motion, dynein, the largest motor protein (Vallee, 1993), harnesses the chemical energy of ATP to produce- through a mechanochemical couple- the mechanical work necessary for cell motility (Hamasaki et al., 1995). It is known that motor proteins play a critical role in cytoskeletal filament function, moving and generating force along cytoplasmic filaments in a uni-directional manner (Howard, 1997).Axonemal dynein is expected to function in a similar manner in the bovine sperm flagellum. A total of 45,000 dynein arms form regularly spaced cross-bridges between each of 9 adjacent circularly-arranged doublet microtubule rods that run internally

throughout the 60 μm length of the sperm flagellum (Linck, 1979). A bending moment is generated at points along the flagellum when dynein arms force microtubules to slide past each other, effectively shortening the length along the inner tubule and inducing curvature. The cyclic attachment and detachment of dynein heads drives the sliding of adjacent microtubules against stiff resistances of the axonemal structures, resulting in the bending of the flagellum. This action gives rise to the quasi-helical rhythmic flagellar motions necessary for sperm movement (Brokaw, 1989; Gibbons, 1981; Gibbons, 1989; Gibbons and Rowe, 1965; Rikmenspoel, 1965; Summers and Gibbons, 1971). Given the small size of the sperm cell's head (9.5 μm x 4.5 μm x 0.75 μm) and tail (60 μm x 0.75 μm x 0.75 μm), the viscous forces dominate inertial forces in the process of swimming for both the head and tail at typical sperm speeds of 27-127 μm/s.

In the present study, we have measured the propulsive force of individual swimming sperm cells (Fig. 1). We used an optical lever equipped with a 4-quadrant photodetector, as used in lateral force (Meyer and Amer, 1990) scanning probe microscopy (Binnig et al., 1986). Individual sperm cells were observed using an integrated optical microscope to "swim up" and adhere to the bottom side of the free end of the cantilever and remain in contact for a period up to several seconds (Fig. 1). Albeit brief, the motive force of a sperm cell (which is pushing against the surrounding viscous medium) mechanically-coupled to the cantilever end, in turn, generates deflections of the calibrated sensor arm thereby allowing nano-scale force *vs.* time measurements to be recorded. Vertical deflections are discriminated from horizontal deflections using the 4-quadrant photodector so that the entire forward propulsive force (perpendicular to the sensor long axis) is measured as a function of time. It should be emphasized that nothing is specifically required to attract sperm cells to the silicon sensor end. The cells contact the cantilever end frequently enough during the course of their normal motion to allow the collection of a large data set of recordings. Previous measurements of the sperm

propulsive force have provided static values for the force, such as the stall force induced by a micropipette (Schmitz et al., 2000) and the escape force from an optical trap (König et al., 1996). The force we have measured is not constant (Fig. 1), and the time dependence of the propulsive force offers new insight into the process of flagellar force generation all the way down to the level of the action of the dynein molecular motors.

Methods

Sperm preparation

Bovine sperm samples were collected throughout the study from the same individual prize bull sired in Tracy, CA by SpermCo. Two sperm preparations were prepared immediately after semen collection in glass test tubes for use in experiments: (1) 5 cc of the raw semen, and (2) 50 cc of a 4:1 semen: sodium citrate mixture. The samples were allowed to equilibrate thermally over a period of approximately 1 hr and then refrigerated at 4ºC until used. The samples were warmed at room temperature 10-15 min prior to use. Raw semen samples were analyzed within 2 hr and citrate-extended samples within 6 hr after collection. Through a side-port, 2-3 µl of diluted sperm were injected into a glass chamber housing the force sensor containing 50 µl of a Tris-saline solution (T/S, 50 mM Tris-HCl, 150 mM NaCl, pH 7.4; 18 Megohm molecular biology grade water; Sigma Chemical, St. Louis, MO). Using an integrated video microscope, sperm cells could be seen swimming into the area of the cantilever sensor within 30 s following injection. The semen samples were diluted 200 fold in T/S.

Force measurements

Cantilevered force sensors made of uncoated silicon (model CSC17, MikroMasch, Tallinn, Estonia) were used to perform the force measurements. The dimensions of

these sensors are as follows: length, 460 μm (±5 μm); width, 50 μm (±3 μm); thickness, 2.0 μm (±0.5 μm). Sensor force constants were determined by the manufacturer using a technique developed by Sader et al., 1999, based on fluid damping of an oscillating sensor. According to the manufacturer, the uncertainty in the calibrated force constant values is less than 10%. The force constants for 6 cantilevers used in these studies were: 50, 57, 105, 141, 150, 261 pN/nm. This study used a Digital Instruments, NanoScope IIIa, MultiMode AFM with NanoScope Extender electronics and version 4.42r4 NanoScope software in Windows NT (Digital Instruments/Veeco Metrology Group, Santa Barbara, CA). The signal to noise performance of this system is optimized with a custom-built vibration isolation apparatus based on an elastomer length that suspends the AFM system's mass with a vertical resonance of 0.5 Hz. A video microscope with long working distance optics of approximately 1 μm two-point resolution was integrated with the AFM allowing a normal view of the sensor during the force measurements. The AFM's piezoelectric scanner was calibrated using NIST-traceable silicon calibration gratings (Silicon-MDT, Moscow, Russia). Vertical steps 24.0 nm, 106 nm and 511 nm in height on the silicon gratings were measured in order to calibrate the scanner in the z-axis. The "E" scanner used has a vertical range of motion of approximately 3 μm. The AFM laser diode was allowed to run for approximately 1 hr before measurements were made. Following laser alignment, the cantilever was allowed to sit in the imaging buffer until thermal drifts were minimized during the thermal equilibration. Optical sensitivity calibrations were then performed against a plane of glass under imaging buffer for each force sensor. Without applying any vertical or lateral scanning or offset voltages to the AFM, and the force sensor completely submersed in the buffer containing live, swimming sperm cells, the motions of the force sensor were monitored in the vertical and horizontal quadrants of the photodetector simultaneously. Typically, 0.5 s scans

were collected. The location of the sperm cell along the length of the cantilever was observed using video microscopy. Force scans used for longitudinal propulsion measurements were from sperm cells interacting with the cantilever at a point within several microns of the free end of the cantilever.

Results

The longitudinal propulsive force exerted by the flagellum of single, swimming bovine sperm cells was determined by monitoring the vertical deflection and horizontal twist of a micromechanical cantilever sensor as a motile sperm cell exerted force against it (Fig. 2). During contact the force generated by an individual, motile sperm could be measured as a function of time. The true force is related to the measured force by

$$F_{true} = \frac{2F_{measured}}{(3\xi^2 - \xi^3)\sin\theta} \qquad (1)$$

where $\xi = x_0 / L$ is the relative position of the sperm, and θ is the angle the sperm propulsion force makes with the cantilever. Here x_0 is the position of the sperm measured from the attachment point of the cantilever of length L. The vertical force is at its maximum value (Fig. 2d) and the cantilever twist is minimized (Fig. 2c) when the sperm swims perpendicularly against the end of the cantilever. This force is significantly higher than the stall (Schmitz et al., 2000) and release (König et al., 1996) forces reported previously for sperm. In contrast to the stall and release forces, the force measured by the cantilever is a direct measure of the propulsive force imparted to the cantilever by the swimming cell. Because the time scale for viscous relaxation and the time scale set by inertia are both sufficiently short, the cantilever system is capable of directly measuring the time dependence of ~10 Hz force oscillations. These time scales

are determined from the equation of motion for the cantilever. The balance of inertial, viscous, elastic and driving forces for a cantilever deflected by an amount *y* is described by the equation

$$\rho A\ddot{y} + 6\eta\dot{y} + 3kL^2 \frac{\partial^4 y}{\partial x^4} + F(t)\delta(x - x_0) = 0 \qquad (2)$$

when the sperm is located at x_0 imparting a force *F(t)*. The dots indicate time derivatives. The density, cross-sectional area and spring constant of the cantilever are ρ, *A* and *k*, respectively. The viscous and inertial response times are then given by:

$$t_{viscous} = 6\eta L / k \quad \text{and} \quad t_{inertia} = \sqrt{3\rho AL / k}\,. \qquad (3)$$

A typical cantilever with k=0.05 N/m, L=460 μm and A=100 μm^2 has response times 55 μs and 60μs that are much shorter than the 0.1 s period of the flagellar motion. Since the response of the cantilever is practically instantaneous, the time dependence of the measurement accurately represents the force exerted on the cantilever as a function of time.

We performed measurements on 12 sperm samples using 6 different force sensors with widely varying calibrated force constants. The measured force amplitudes and frequencies are plotted in Fig. 3 for the 6 different sensors. Each point is labeled with the corresponding force constant and deflection. Values of forces ranging from 7.35 nN to 14.36 nN were observed. As evident in Fig. 3 there is no correlation between the force exerted in a single pulse and the beat frequency. For example, the pulsating vertical deflections observed with a 50 pN/nm cantilever were 160 nm, while a cantilever of 195 pN/nm recorded 45 nm pulsating deflections of a 20% lower frequency. Despite the large difference in deflections, the measured forces differed by less than 10%. Similar forces were obtained for sperm cells from raw semen or after

dilution in citrate buffer. An average force of 9.88 nN represents the maximum propulsive force generated each time the flagellum moves through a single beat cycle. The lower limit for the energy required to produce the force associated with a single flagellar pulse may be approximated by the maximum elastic energy stored in the cantilever during a pulse. Using $Work = \frac{1}{2} k y_{tip}^2$, the energy required for a sperm cell to displace the sensor to its peak deflection was calculated to be 4.6 x 10^{-16} J, equivalent to the energy produced by the hydrolysis of ~5500 ATP molecules. This value is typical, although it should be noted that while the force measured was largely independent of the beat frequency and cantilever spring constant, the work done by the sperm, $Work = \frac{1}{2} F^2 / k$, did vary with the spring constant, ranging from 2.44 x 10^{-16} J to 8.60 x 10^{-16} J.

Discussion

While precise modeling of the motion of the flagellum is beyond the scope of this current effort, it is important to assess whether the measured forces are consistent with what is known about motor protein activity *in vitro*. As a first step, we have used the results obtained from the force and energy measurements to estimate the minimum number of dynein arms involved in flagellar function based on the amount of work carried out during the force pulse and an assumption of one active ATPase per dynein head. If each of these ~5,500 ATPases hydrolyzes 1 ATP molecule during a 50 ms pulse, as consistent with the enzymatic properties reported for dynein (Lark et al., 1994), the number of dynein heads involved in forward propulsion should be equal to the number of ATP molecules hydrolyzed, i.e. ~5500. Since there are known to be on average 2.14 dynein heads per outer or inner dynein arm in the bovine sperm flagellum

(Schmitz et al., 2000), this then means that ~2600 dynein arms are actively involved in force generation as measured in the propulsive force-pulse. These active dynein arms, which represent only ~6% of the total dynein arms present in the sperm tail (~45,000), are equivalent to roughly ½ the number of arms located along a single microtubule doublet row, which runs the length of the bovine sperm tail. Since the coupling efficiency between the flagellum and the surrounding fluid is sure to result in some energy loss during the propulsion, we cannot eliminate the possibility that our analysis has underrepresented the number of active dyneins involved. However, the vast majority of energy loss appears to occur during the time the bulky sperm head is being pushed relatively long distances through the low Reynolds number environment (Konig et al., 1996)

Using the number of active dynein arms, we are able to calculate the mechanochemical coupling between molecular dynein and ATP. We report the coupling at each active dynein head to be 2.2 ± 1.0 pN/ATP and at each active dynein arm 3.9 pN/2.14 ATP. A force of ~4 pN per dynein arm, measured using live sperm, agrees well with previous *in vitro* force measurements using isolated dynein arms, as well as studies on other motor proteins. Force measurements conducted with microneedles and optical traps have indicated the force exerted by a single dynein arm is on the order of 1-6 pN (Kamimura and Takahashi, 1981; Shingyoji et al., 1998). This is similar to the forces (3-7 pN) that have been reported for other motor proteins, such as kinesin and myosin (Higuchi et al., 1997; Svoboda and Block, 1994; Ishijima et al., 1994; Finer et al., 1994). We note that the value of the mechanochemical couple is simply related to the deflection of the cantilever in this measurement: $f_0 = 2R/u$ where R (= 83 pN-nm/ATP) is the energy per ATP and u is the cantilever deflection.

The results of these studies also provide information about how this dynein-driven sliding of the microtubules relates to the bending of the flagellum. The bovine flagellar waveform has a period equivalent to the entire length of the tail (~60 μm). The flagellum is known to bend through an angle of roughly $\Delta\theta=90^{o}$ and back in the course of its motion, and the diameter of the axoneme is d=96 nm (Woolley, 1990). The geometry of the arc then dictates that the length one half of the axoneme would need to slide relative to the other is a total of ($\Delta\theta$ d) ~160 nm each half-period (50 ms). Using this distance, the average sliding velocity is calculated to be 3.1 μm/s, a value that is consistent with published results for sea urchin sperm (Yamada et al., 1998; Yano and Miki-Noumura, 1980).

The total sliding distance of 160 nm is only 7 to 40 times the published value for the molecular sliding distance reported previously per arm, which is in the range of 4 to 24 nm (Hamasaki et al., 1995). We have inferred that a total of ~2600 dynein arms are active for some duration during the force-pulse, and so hundreds of dynein arms must be head-attached and working in unison to generate force during numerous sliding events throughout a force-pulse. A working distance of 12 nm corresponds to 13 independent sliding events (to give a total sliding distance of 160 nm) each involving ~200 dynein arms (out of the 2600 available) active at any one time during the force-pulse. Using these numbers, the ratio of working distance to sliding velocity (3.8×10^{-2} s) multiplied by the rate of ATP hydrolysis ($20\ s^{-1}$) provides an estimate of the duty ratio. The duty ratio determined in this study, 0.08, is consistent with previous *in vitro* findings that suggest the axonemal dynein is a low duty motor (Howard, 1997; Hamasaki et al., 1995).

The force exerted by a sperm cell as it swims through aqueous buffer has been measured previously using an optical trap (König et al., 1996). After trapping the cell with a focused infrared laser, the force was measured by lowering the power of the calibrated laser trap until the cell could escape the trap. The 10,000 pN propulsive force we report for bovine sperm is ~200 times greater than the 44 +/- 20 pN swimming force for human sperm as measured with the optical trap. There are no apparent changes in the frequency or amplitude of the flagellar motion when the sperm contacts the cantilever; neither were there reported changes in the sperm behavior due to the optical trap. Variations between the two species are expected to be small. One apparent difference, however, is that the sperm head is essentially stationary on the cantilever, whereas the optical trap force is distributed across the entire sperm and the head is free to move. This large disparity suggests that sperm motility in liquid is a very inefficient process with less than 0.5% of the force used for longitudinal propulsion is translated into the force of a swimming sperm cell. The enormous energy cost of moving the sperm through liquid appears to be outweighed by its evolutionary benefit and this may reflect that the sperm flagella has not been optimized for motion through aqueous buffer but rather for penetrating more viscous media and to performing other functions, such as applying large forces once the sperm contacts the surface of the oocyte.

In conclusion, the measured time dependence of the force, shown in Fig. 2d, provides information that can be used to identify, in a quantitative manner, different aspects of the process that lead to the generation of the propulsion force. The data contain information at each instant of the flagellar motion that can be used to determine how the dynein-driven force is transformed into the elastic force of flagellar bending, and how that force in turn is coupled to the surrounding fluid (i.e., the viscous force) to provide

forward propulsion. Force produced by the flagellum increases monotonically to a peak value of nearly 10 nN over a period of 25 ms and then monotonically decreases in time nearly symmetrically. The work performed by the force-pulse is 4.6×10^{-16} J equivalent to the energy released from the hydrolysis of 5500 ATP molecules corresponding to a force quantum of 3.9 pN from the action of each dynein arm, and a mechanochemical coupling of 2.2 pN/ATP per dynein head. The results also suggest that as few as 6% of all dynein arms present in the axoneme are actively involved in any one propulsive force-pulse event.

The data we have presented provide the basis for a more detailed understanding of the sequence of molecular events that contribute to propulsion at the cellular level (a level within which viscous forces dominate inertial forces). Understanding how to control propulsion at the nano-level has implications not only in assessing cell motility and sperm fertilizing potential but also in the development of actively transportable nanodevices and sensors via biomimetic nano-motors for Nanomedicine.

Acknowledgments: We gratefully acknowledge Prof. Calvin Quate for a thorough critical review of the manuscript and many helpful suggestions. We also thank J. Silveira for his fine technical support. This work was performed through support from Biometrology to M.J.A.; and to R.E.R., M.W.M. and R.B. under the auspices of the US Dept. of Energy by the Lawrence Livermore National Laboratory under Contract No. DE-AC52-07NA27344.

References

1. Binnig G, Quate CF, Gerber C. Atomic force microscope. Phys Rev Lett 1986; 56: 930-33.

2. Brokaw CJ. Direct measurement of sliding between outer doublet microtubules in swimming sperm flagella. Science 1989; 243:1593-96.

3. Finer JT, Simmons RM, Spudich JA. Single Mysoin Molecular Mechanics: Piconewtons Forces and Nanometer Steps. Nature 1994; 368:113-19.

4. Gibbons IR, Rowe A. Dynein: a protein with adenosine triphosphatase activity from cilia. Science 1965; 149:424-25.

5. Gibbons IR. Cilia and flagella of eukaryotes. J Cell Biol 1981; 91:1071-1245.

6. Gibbons IR. In: Cell Movement: The Dynein ATPases. P. Satir, and I.R. Gibbons, editors. Liss, New York; 1989, p. 3-24.

7. Hamasaki T, Holwill ME, Barkalow K, Satir P. Mechanochemical aspects of axonemal dynein activity studied by in vitro microtubule translocations. Biophys J 1995; 69:2569-79.

8. Higuchi H, Muto E, Inoue Y, Yanagida T. Kinetics of force generation of single kinesin molecules activated by photolysis of caged ATP. Proc Natl Acad Sci 1997; 94:4359-4400.

9. Howard, J Molecular motors: structural adaptations to cellular functions. Nature 1997; 389:561-68.

10. Ishijima A, Harada Y, Kojima H, Funatsu T, Higuchi H, Yanagida T. Single-molecule analysis of the actomyosin motor using nano-manipulation. Biochem Biophys Res Commun 1994; 199:1057-63.

11. Kamimura S, Takahashi K. Direct measurement of the force of microtubule sliding in flagella. Nature 1981; 293:566-68.

12. König, K, Svaasand L, Liu Y, Sonek G, Patrizio Y, Tadir M, et al. Determination of motility forces of human spermatozoa using an 800 nm optical trap. Cell Molec Biol 1996; 42:501-09.

13. Lark E, Omoto CK, Schumaker MK. Functional multiplicity of motor molecules revealed by a simple kinetic analysis. Biophys J 1994; 67:1134-40.

14. Linck RW. In: The Spermatozoon. D.W. Fawcett, and J.M. Bedford, editors. Urban and Schwarzenberg, Baltimore. 1979, p. 99-105.

15. Lindemann CB. A 'geometric clutch' hypothesis to explain oscillations of the axoneme of cilia and flagella. J Theor Biol 1994; 168, 175-189.

16. Meyer G, Amer NM. Simultaneous measurement of lateral and normal forces with an optical-beam-deflection atomic force microscope. Appl Phys Lett 1990; 57:2089-91.

17. Rikmenspoel R. The tail movement of bull spermatozoa. Observations and model calculations. Biophys J 1965; 5:365-92.

18. Sader J, Chon J, Mulvaney P. Calibration of rectangular atomic force microscope cantilevers. Rev Sci Instr 1999; 70:3967-69.

19. Satir P. The generation of ciliary motion. J Protozool 1984; 31:8-12.

20. Schmitz KA, Holcomb-Wygle DL, Oberski DO, Lindemann CB. Measurement of the force produced by an intact bull sperm flagellum in isometric arrest and estimation of the dynein stall force. Biophys J 2000; 79:468-78.

21. Shingyoji C, Higuchi H, Yoshimura M, Katayama E, Yanagida T. Dynein arms are oscillating force generators. 1998; Nature 393:711-14.

22. Svoboda K, Block SM. Force and velocity measured for single kinesin molecules. Cell 1994; 77: 773-84.

23. Summers KE, Gibbons IR. ATP-induced sliding of tubules in trypsin-treated flagella of sea-urchin sperm. Proc Natl Acad Sci USA 1971; 68:3092-96.

24. Vallee RB. Molecular analysis of the microtubule motor dynein. Proc Natl Acad Sci USA 1993; 90:8769-72.

25. Woolley D. In: Controls of Sperm Motility: Biological and Clinical Aspects. C. Gagnon, editor. CRC Press, Boca Raton, FL. 1990, p. 34-35.

26. Yamada A, Yamaga T, Sakakibara H, Nakayama H, Oiwa K. Unidirectional movement of fluorescent microtubules on rows of dynein arms of disintegrated axonemes. J Cell Sci 1998; 111:93-98.

27. Yano Y, Miki-Noumura T. Sliding velocity between outerdoublet microtubules of sea-urchin sperm axonemes. J. Cell Sci 1980; 44:169-186.

Figure 1: Vertical deflection of the force sensor vs. time records an individual sperm cell contacting and then swimming against the sensor (with mechanical coupling). Fresh semen was diluted 200-fold in tris-saline buffer pH 7.4 and injected into a 50 µl fluid chamber containing a calibrated (Sader et al., 1999) force sensor 460 µm in length. The propulsive forces of the sperm cell are represented in a regular oscillating pattern coinciding with the beat frequency of the flagellum. In all cases the reported longitudinal force is calculated from oscillations in the flat region of the scan (*2.31- 2.97 s*) after any initial transient has vanished.

Figure 2: Force measurement and determination of the force vector alignment. Sensor movements in the (*a,c*) horizontal and (*b,d*) vertical planes were recorded simultaneously for two different sperm cells (*a,b* and *c,d*). The horizontal signal records twisting motions of the cantilevered sensor with spring constant 195 pN/nm. The vertical signal records the up/down bending of the sensor. When (*d*) the vertical motions are maximal and (*c*) the twisting motions of the rectangular sensor are minimal, the force of the forward propulsion is measured as the amplitude of the vertical signal. These data are used to calculate the propulsion force and energy (see text). If the sperm cell is misaligned and not swimming in the vertical plane of the sensor, then (*a*) the horizontal signal is relatively strong, and (*b*) the vertical signal weak.

Figure 3: The longitudinal propulsive forces measured using 6 different force sensors (*k= 50-261 pN/nm*) cluster near 9.88 nN (*7.35- 14.36 nN*) regardless of beat frequency (*3.5- 19.5 Hz*). The force constant (*k,* in pN/nm) and vertical displacement (y_{tip}, in nm), respectively, are provided adjacent to the data markers (*squares*) for the sensor used for

the measurement. The datum with spring constant *195* pN/nm corresponds to curve (*d*) in Fig. 2.

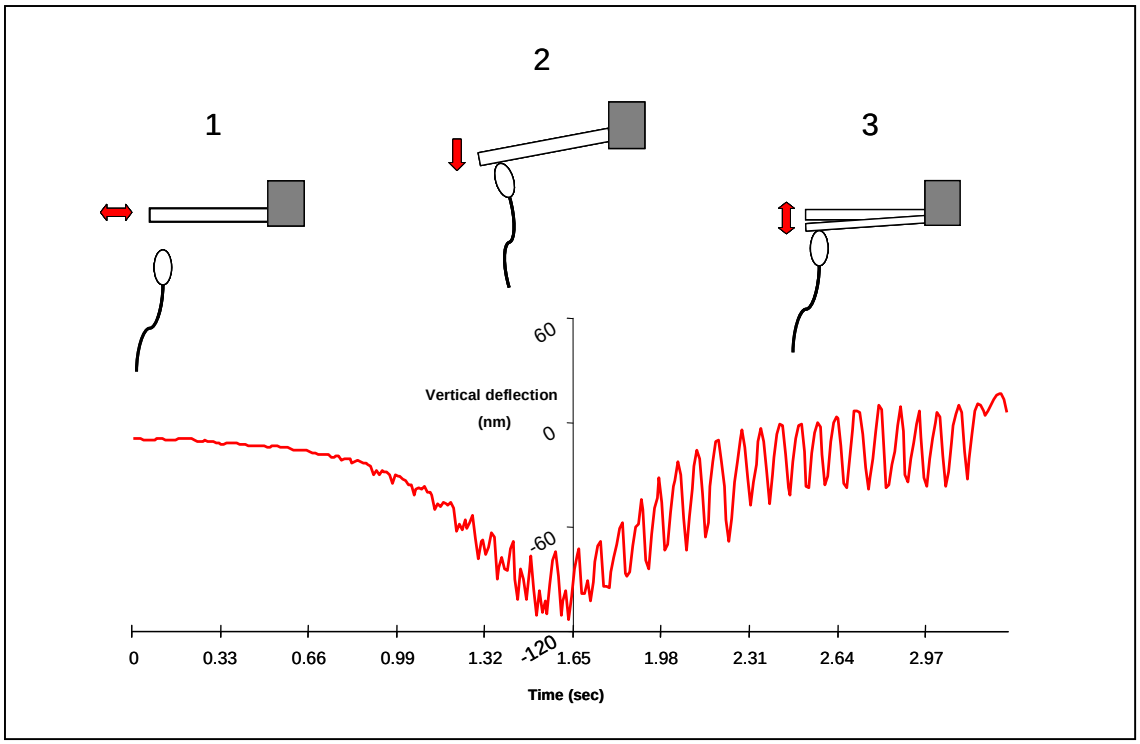
1
2
3
60
Vertical deflection
(nm)
0
-60
-120
0
0.33
0.66
0.99
1.32
1.65
1.98
2.31
2.64
2.97
Time (sec)

Fig. 1

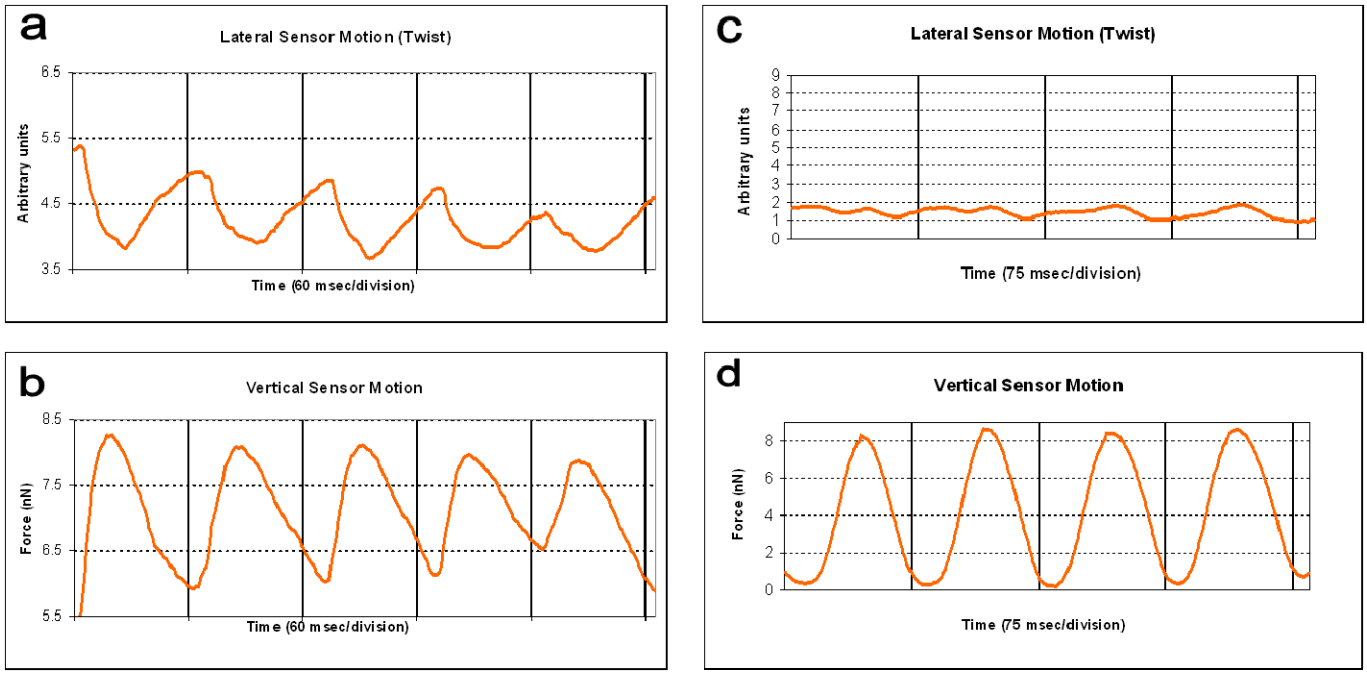
a
Lateral Sensor Motion (Twist)
Arbitrary units
6.5
5.5
4.5
3.5
Time (60 msec/division)
c
Lateral Sensor Motion (Twist)
Arbitrary units
9
8
7
6
5
4
3
2
1
0
Time (75 msec/division)
b
Vertical Sensor Motion
Force (nN)
8.5
7.5
6.5
5.5
Time (60 msec/division)
d
Vertical Sensor Motion
Force (nN)
8
6
4
2
0
Time (75 msec/division)

Fig. 2

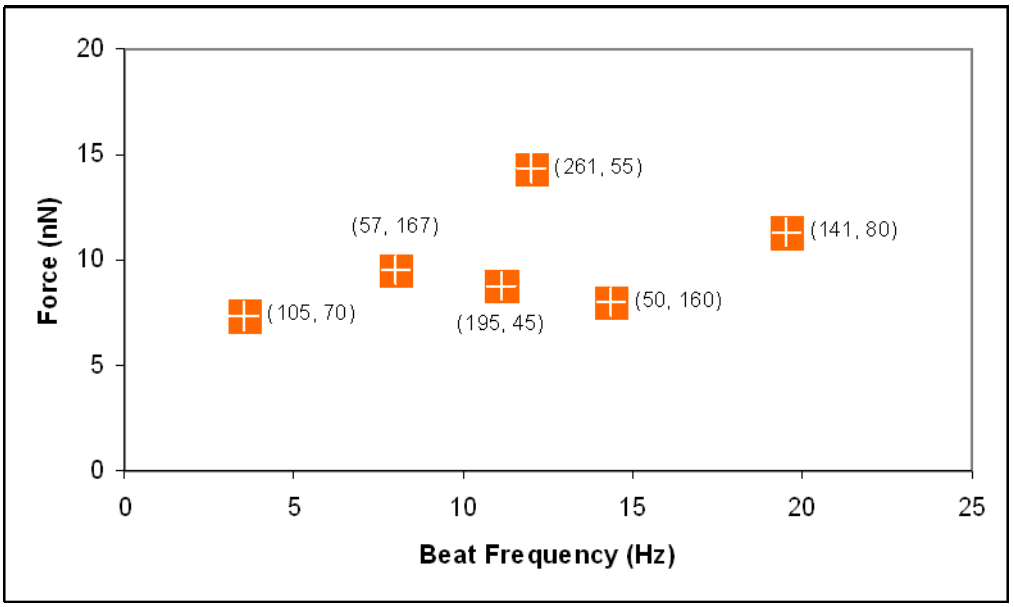
20
15
10
5
0
Force (nN)
0
5
10
15
20
25
Beat Frequency (Hz)
(261, 55)
(57, 167)
(141, 80)
(105, 70)
(195, 45)
(50, 160)

Fig. 3